INTERNATIONAL JOURNAL OF HYDROGEN ENERGY 40 (2015) 6672–6680

Available online at www.sciencedirect.com

ScienceDirect

journal homepage: www.elsevier.com/locate/he

Experimental study of cell reversal of a high temperature polymer electrolyte membrane fuel cell caused by H_2 starvation

Fan Zhou[*], *Søren Juhl Andreasen*, *Søren Knudsen Kær*

Department of Energy Technology, Aalborg University, Pontoppidanstræde 101, 9220 Aalborg East, Denmark

ARTICLE INFO

Article history:
Received 24 December 2014
Received in revised form
13 March 2015
Accepted 27 March 2015
Available online 15 April 2015

Keywords:
H_2 starvation
HT-PEM fuel cell
Cell reversal
Current density distribution

ABSTRACT

Operation under fuel starvation has been proved to be harmful to the fuel cell by causing severe and irreversible degradation. To characterize the behaviors of the high temperature PEM fuel cell under fuel starvation conditions, the cell voltage and local current density is measured simultaneously under different H_2 stoichiometries below 1.0 and at different current loads. The experimental results show that the cell voltage decreases promptly when the H_2 stoichiometry decreases to below 1.0. Negative cell voltage can be observed which indicates cell reversal. The local current density starts to diverge when the cell voltage decreases. In the H_2 upstream regions the current densities show an increasing trend, while those in the H_2 downstream regions show a decreasing trend. Consequently, the current density distribution becomes very uneven. The current density is the highest in the upstream regions, decreasing along the flow channel direction, becoming the lowest in the downstream regions. In addition, the CO_2 and even the O_2 can be detected in the anode exhaust under fuel starvation conditions, confirming the occurring of carbon corrosion and water electrolysis reactions. With lower H_2 stoichiometry and higher current load, the cell voltage decrease rate is higher and the cell reversal is more severe. Higher CO_2 concentration in anode exhaust is measured under these conditions, suggesting the degradation is more severe.

Introduction

High temperature (HT) polymer electrolyte membrane (PEM) fuel cells of which the operating temperature in the range of 130–180 °C is regarded as a promising clean energy power source for both automotive and stationary applications. This type of fuel cell employs a polybenzimidazole (PBI) membrane doped with phosphoric acid (H_3PO_4) as the electrolyte [1]. Higher operating temperature and zero electro-osmotic drag coefficient of the PBI membrane bring the HT-PEM fuel cell some advantages over its low temperature counterpart, such as simpler water and heat management and higher tolerance to impurities in the fuel [2]. In recently years many works have attributed to the development of high temperature PEM fuel cells. Su et al. [3,4] optimized the structure of gas diffusion layer and catalyst layer for the high temperature PEM fuel cells to improve the cell performance. Yan et al. [5] managed to

* *Corresponding author*. Tel.: +45 29632214.
E-mail address: fzh@et.aau.dk (F. Zhou).
http://dx.doi.org/10.1016/j.ijhydene.2015.03.148

fabricate a Poly(2,5-benzimidazole) (ABPBI)-based gas diffusion electrode with single step and demonstrate its MEA for high temperature PEM fuel cell operation. However there are still some disadvantages of the high temperature PEM fuel cells which need to be solved, for example, the long start-up time because of high operating temperature [6] and mass transfer limitation because of the presence of phosphoric acid in catalyst layer [7]. Moreover, relatively high performance decay rate and limited lifetime are also the barriers for the HT-PEM fuel cell achieving successful commercialization.

Fuel starvation, which can refer to undersupply of hydrogen (H_2) in the anode during fuel cell operation, is proved can result in severe and irreversible damages to PEM the fuel cell [8–11]. The fuel starvation can be caused by many factors [12]: uneven gas distribution between different cells within a stack or different regions of a single cell, channel blocked by flooding, fault in control of gas supply system and sudden increase in current load. For PBI/H_3PO_4 high temperature PEM fuel cells, improper distribution of phosphoric acid in the catalyst layer during the MEA manufacturing or break-in process can also result in local H_2 starvation because of local catalyst flooding by acid [13]. When the fuel cell is starved of H_2, the consequence can be severe. Local anode potential increase sharply in regions where the H_2 is depleted, resulting in severe cell reversal [14]. Existence of O_2 and CO_2 in anode exhaust gas observed by Liang et al. [11] under H_2 starvation conditions proves that the water electrolysis and carbon corrosion reactions take place at the anode side when the fuel cell is starved of H_2. Under this condition the carbon corrosion is enhanced by the high potential in anode, leading to the irreversible loss in the electrochemical catalyst surface area (ECSA) [8]. Therefore, to achieve durability targets of PEM fuel cells, effects of gas starvation on transient and long-term performance are worth investigating.

During the fuel starvations operation, the current density and temperature distribution become very uneven because of local depletion of H_2, which can accelerate the degradation of the fuel cell. Measurement of local current density distribution during gas starvation operation provides an effective diagnostic tool to investigate the local behavior of the fuel cell and develop optimization strategies for mitigation [15]. Dynamic behaviors of local current density of a low temperature PEM fuel cell under gas starvations conditions have been investigated by some researchers [11,16,17]. Liang et al. [11] investigated the transient response of current distribution under different H_2 starvation conditions with H_2 stoichiometries of 1.09, 0.91, 0.73, and 0.55. They found that the current distributions were significantly uneven under different H_2 starvation conditions. Zhang et al. [16] investigated the air starvation and H_2 starvation under current controlled mode and voltage controlled mode. Local current density and temperature distributions were measured during the tests. In current control mode, cell voltage decreased quickly during gas starvation. Current density and temperature distribution were quite uneven and dependent on the location along the flow channel. On the other hand, local current density and temperature did not respond drastically during gas starvation in voltage control mode, which indicated it was a safer operation mode. Yu et al. [17] investigated the current distribution of a fuel cell under gas starvation at different current densities. The experimental results showed that the current density was uniform at low current load and became obviously non-uniform at high current load. The current at segments near the gas inlet were higher than at segments near the gas outlet. More severe non-uniform current distribution can be observed at H_2 starvation, compared to air starvation. The fuel starvation on phosphoric acid fuel cell (PAFC), of which electrolyte and catalyst layer is similar to those of PBI/H_3PO_4 HT-PEM fuel cell, has been investigated by several researchers [18,19]. Mitsuda and Murahashi [18] observed the CO and CO_2 in the fuel exhaust gas under fuel starvation condition, confirming the occurrence of carbon corrosion in the anode component. Song et al. [19] studied the effect of gas starvation on the cell performance of PAFC. They observed 5 mV-loss in cell voltage after H_2 starvation operation. Recently, a stressed degradation test of a PBI-based high temperature PEM fuel cell under H_2 starvation condition has been conducted by Zhou et al. [20]. A significant performance loss can be observed after a short period when the fuel cell was exposed to H_2 starvation condition, which demonstrates that the H_2 starvation is detrimental to the high temperature PEM fuel cell. Therefore the behaviors of the fuel cell under H_2 starvation are worth investigating to better understand the influence of H_2 starvation on operation of the fuel cell.

In this work the dynamic behaviors of cell voltage and local current density of a PBI/H_3PO_4 high temperature PEM fuel cell are measured simultaneously under different H_2 starvation conditions. The effects of current load and H_2 starvation degree on the behaviors of the fuel cell are investigated. A segmented sensor plate mounted behind the cathode flow field plate was employed to measure the current density distribution during the experiments. The experimental results from this work can help to gain insights into the operation of the fuel cell under H_2 starvation conditions.

Experimental setup

Hardware setup

A commercially available MEA Dapozol® G77 produced by Danish Power System® with active area of 49 cm^2 (7 cm × 7 cm) is chosen in this work. This MEA is based on a PBI/H_3PO_4 membrane with a thickness of 80 μm and a doping level around 9 (H_3PO_4 molecules per PBI unit). The platinum loading on both anode and cathode electrodes is 1.6 mg/cm^2. The thickness of the gas diffusion layer is 250 μm. The MEA is inserted between two graphite bipolar plates with double serpentine flow channels, which are of the same geometric properties on two plates. PTFE gaskets with thickness of 250 μm are adopted to guarantee the gas tightness and proper compression of the MEA during assembling. Two stainless steel plates embedded with four heaters (4 × 57 W) on each plate are used as the end plates for assembly. To measure the current density distribution, a sensor plate with 100 sensors (10 × 10) evenly distributed is installed between the graphite plate and the stainless steel plate in cathode side. The detailed measurement methodology will be introduced in the next section. The scheme of the single cell setup is illustrated in Fig. 1.

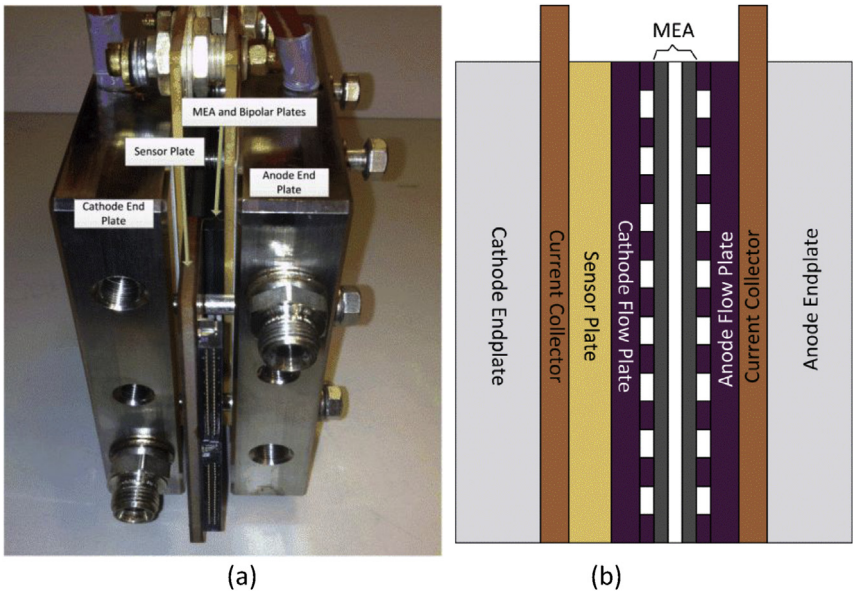

Fig. 1 – Photograph (a) and schematic plot (b) of the single fuel cell setup with segmented sensor plate for current density distribution measurement.

The MEA is tested on an automated fuel cell test station FCATS G60 (Greenlight Innovation®, Canada), which can control the operating parameters of the fuel cell, including stoichiometries and back pressure of anode and cathode, cell temperature and current load. Additionally it provides the function of feeding pure N_2 into anode and cathode pipe for gas mixing and evacuating residual H_2 and air after shut down. In this work, unhumidified air was employed as oxidant on the cathode, and unhumidified H_2 and N_2 mixture (70% H_2 and 30% N_2 in volume) was employed on the anode. Liang et al. [10] reported the 'vacuum effect' that H_2 was drawn back into the anode flow channel from the manifold in a fuel cell stack under fuel starvation conditions. In this work, the long fuel exhaust pipe can act as the manifold in a fuel cell stack. Therefore the H_2/N_2 mixture was adopted to avoid the 'vacuum effect'. For all experiments the cell stood upright, and the air flowed from the top to the bottom while the H_2/N_2 mixture flowed from the bottom to the top, indicating a counter flow configuration. A quadrupole mass spectrometer (OmniStar GDS 301, Pfeiffer Vacuum) was adopted to analyzer the composition of the anode exhaust gas.

Current density distribution measurement

The technique to measure the current density distribution on the MEA surface is to insert a sensor plate with 100 segments between cathode bipolar plate and current collector plate. The setup is the current scan lin (Test50 HT) developed by S++ company. The measurement principle is based on the dependence of the permeability of soft magnetic material on magnetic field strength and temperature. On each segment of the sensor plate there is a core made of soft magnetic material and several coils which is used to measure the current flowing through this part of plate. By connecting a data acquisition board to the sensor plate, the measured local current values can be stored in a computer, and the current density distribution map can be easily plotted by combining the local current density value and the position of the segment. A minimum interval of 0.5 s is allowed for the current density distribution measurement, ensuring that the dynamic characteristic of local current density can be recorded. Fig. 2 illustrates the scheme of the segmented sensor plate, flow field in anode and cathode and the gas flow configuration.

With this segmented sensor plate, current density distribution can be measured without segmenting the MEA, electrodes or the bipolar plates, thus operation of the cell and the current density distribution would not be interrupted. However it should be mentioned that the accuracy of the measurement can be affected by lateral current existing in the bipolar plates, although relatively thin bipolar plates (2 mm) have been adopted to minimize the measurement error.

Experimental procedure

Once the single cell setup with current density sensor plate was assembled and mounted on the fuel cell test station, it was operated at 160 °C and 200 mA/cm^2 for 120 h for break-in, with stoichiometrics of 2 and 4 in the anode and cathode, respectively. During the break-in, the cell voltage increased gradually, and a maximum and stable cell voltage indicated the completion of the break-in. After that, the operating temperature was set at 150 °C and both the anode and cathode stoichiometries were set at 3.

To mimic the operating conditions where the fuel cell is starved of fuel, experiments were conducted under low anode gas flow rate conditions. The anode stoichiometry decreased from 3 to 0.8 and 0.4 in each experiment while the air stoichiometry was remained at 3. The H_2 flow rate in the anode feed stream was determined according to the anode stoichiometry, while the N_2 flow rate was calculated according to the volume fraction of H_2 (70 %vol) and N_2 (30 %vol) in the anode

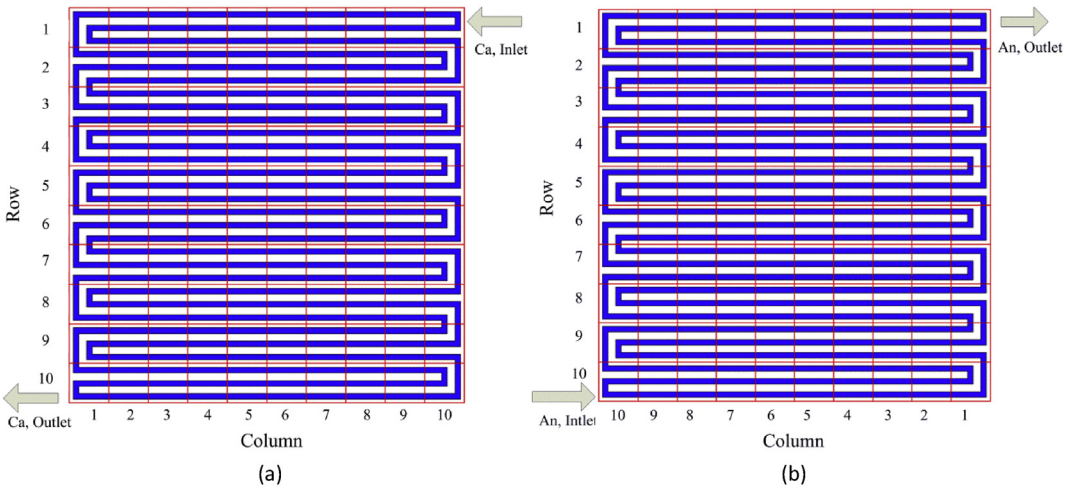

Fig. 2 – Scheme of segmented sensor plate (red line) and flow channel (blue line) and configuration of gas flow in (a) cathode; (b) anode. (For interpretation of the references to color in this figure legend, the reader is referred to the web version of this article.)

feed gas. The total flow rate of anode feed stream was the sum of H_2 flow rate and N_2 flow rate.

All tests were performed at two different current loads (10 A and 20 A) to investigate the effect of current load to the starvation of the fuel cell. In all experiments the operating temperature was kept at 150 °C. The detailed operating conditions for all the experiments are listed in Table 1.

Results and discussions

Behaviors of the fuel cell under H_2 starvation conditions

Fig. 3 shows the change in the voltage of the fuel cell and current density values in different regions when the H_2 stoichiometry decreased from 3.0 to 0.8 which triggers the fuel starvation of the fuel cell. In Fig. 3 the notation 'i_Rn' (n = 1, 2, 3 … 10) represents the average current density in each row of the segments as illustrated in Fig. 2. From the configuration of the flow channel and the segments of the sensor plate, it can be seen that the notion from 'i_R10' to 'i_R1' represents the average current density in upstream region to downstream region, along the flow channel. The 0 s in Fig. 3 indicates the moment when the H_2 stoichiometry decreased. In the first 5 s the cell voltage remains unchanged. Although the H_2 flow rate in the anode inlet has dropped to a value that can cause fuel shortage during this period, residual H_2 in the flow channel and gas diffusion layer can still react to maintain the current and cell voltage. After the first period, the cell voltage shows a dramatic decreasing trend which suggests the residual H_2 has been depleted. In the H_2 starvation condition, the H_2 flow rate is lower than the H_2 consumption rate, which causes the H_2 depletion in the anode of the fuel cell. At 19 s, the cell voltage decreases to 0 V and then becomes negative, indicating a change in the cell polarity. The cell reversal caused by H_2 starvation in low temperature PEM fuel cells has been reported in some works, and it was attributed to the increasing anode potential which became higher than the cathode potential under H_2 starvation conditions [9,11]. Since the materials of the anode catalyst layer is similar for Nafion membrane based low temperature PEM fuel cell and PBI/H_3PO_4 high temperature PEM fuel cell, it can be inferred that the anode potential increases under H_2 starvation condition in this study, resulting in cell reversal. In a fuel cell, the anode

Table 1 – Operating conditions for the fuel cell during H_2 starvation experiments.

Experiment no.	Current load (A)	H_2 stoichiometry	Air stoichiometry
1	10	0.8	3
2	10	0.4	3
3	20	0.8	3
4	20	0.4	3

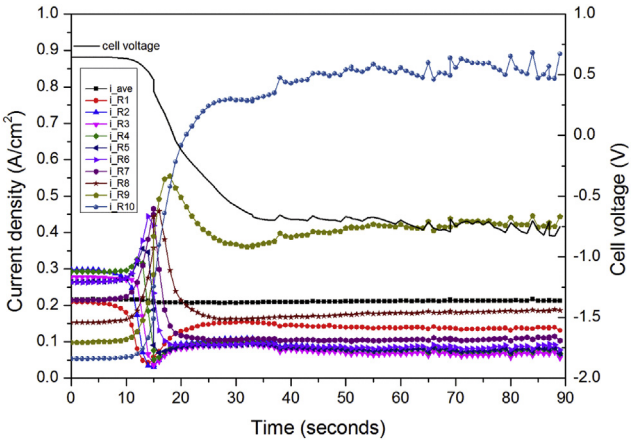

Fig. 3 – Dynamic response of cell voltage and local current density when H_2 stoichiometry decreased from 3.0 to 0.8 with the current load of 10 A.

and cathode potential (E_a, E_c) can be written as the following equations [21]:

$$E_a = E_{eq,a} + \eta_a$$

$$E_c = E_{eq,c} - \eta_c$$

where $E_{eq,a}$ and $E_{eq,c}$ are equivalent potential of anode and cathode, and η_a and η_c are overpotential which could be induced by charge transfer resistance and mass transfer resistance in anode and cathode, respectively. When the anode is starved of H_2, the decrease in H_2 partial pressure at the catalyst surface can result in an increase in the mass transport resistance, leading to an increase in the anode overpotential. In the meantime the cathode potential is not significantly affected because the cathode is supplied with sufficient oxygen. Therefore the anode potential increases under an H_2 starvation condition which is the reason for the dramatic drop in cell voltage. When the anode potential becomes higher than the cathode potential, the cell reversal occurs. The negative cell voltage suggests that the operation mode of the fuel cell switches from the 'generator mode' to the 'load mode'. That is to say the fuel cell consumes energy provided by the auxiliary power supply when the polarity is reserved, rather than generating energy as under the normal operating condition. In the real application, the energy could be provided by other cells in a stack or other stacks when the stacks were connected electrically. With further increase in the anode overpotential, the cell voltage decreased and reached the lowest level until the new equilibrium was established. Under H_2 starvation condition there is not enough H_2 to maintain to current value, thus carbon corrosion and even water electrolysis reactions would occur which provides electrons and protons to compensate the current value.

The standard potential for carbon corrosion reaction is 0.207 V vs RHE, which is usually lower than the positive electrode potential when the fuel cell is under normal operating condition. The carbon corrosion rate is low at typical operating condition. However, the high anode potential caused by the H_2 starvation can accelerate the carbon corrosion rate sharply, resulting in severe degradation on the anode side. The standard potential for water electrolysis reaction is 1.229 V vs RHE, which is higher than the electrodes potential under normal operating conditions. With severe H_2 starvation which brings about an extremely high anode potential could result in the water electrolysis reaction. By analyzing the anode exhaust composition through an in-situ gas mass spectrometer, it can be found that the anode exhaust consisted of N_2, CO_2 at the H_2 stoichiometry of 0.8, as shown in Fig. 4. There is no H_2 detected in the anode exhaust which suggests the H_2 is consumed in the anode of the fuel cell. The N_2 comes from the anode inlet gas because it does not react with anything in the anode. The CO_2 is generated by the carbon corrosion which confirms H_2 starvation could result in high anode potential and consequently carbon corrosion in anode of the fuel cell. There is no O_2 detected in this condition, indicating the anode potential is not high enough to trigger the water electrolysis reaction.

The change in the current density in this experiment is related to the change in the cell voltage, as shown in Fig. 3. In the first 5 s the current densities in all regions remain constant when the cell voltage is stable. When the cell voltage starts to decrease in this experiment, the current density values in different regions also starts to diverge. The current densities in downstream regions (R1, R2 and R3) decreases, while in other regions (R4 to R10) show the opposite trend. As the H_2 stoichiometry decreases below 1.0, the H_2 depletes in the downstream regions, resulting in the increase in the mass transfer resistance in these regions. Therefore the current tends to flow through regions with lower resistance which explains the increase in current density in the upstream regions. As the cell voltage decreases further, the current density in central part of the flow field (R4 to R9) shows the decrease trend successively from the region near the fuel inlet (R4) to the region near the fuel outlet (R9). This suggests that the H_2 depletion spreads from the downstream regions to the upstream regions. Only in the region nearest to the fuel inlet (R10) the current density keeps increasing. When the cell voltage decreases to the lowest level and remains stable, the current densities in all regions stops diverging and reaches the stable level as well.

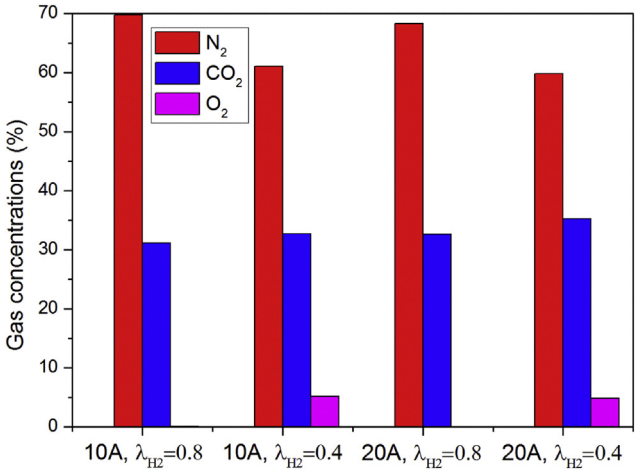

Fig. 4 – Gas composition of anode exhaust under different operating conditions.

In work of Zhang et al. [16] the change in local current density was measured in H_2 starvation process without the cell reversal. In that experiment there was no auxiliary power supply to provide power to the fuel cell under cell reversal condition, thus the cell voltage can only decrease to 0 V. In this work the change in the cell voltage and local current density are similar to those under H_2 starvation conditions without cell reversal. The differences lie in that in this work the lowest cell voltage is negative and the divergence in local current density in different regions is more severe. This suggests that the cell reversal under H_2 starvation condition brings about more heterogenous current density distribution. In addition, with an auxiliary power supply connecting with the fuel cell, the performance of a single cell in a fuel cell stack under H_2 starvation conditions can be further investigated in this work.

The current density distributions of the fuel cell in different time during the experiment are illustrated in Fig. 5. The current density distribution at the beginning of the

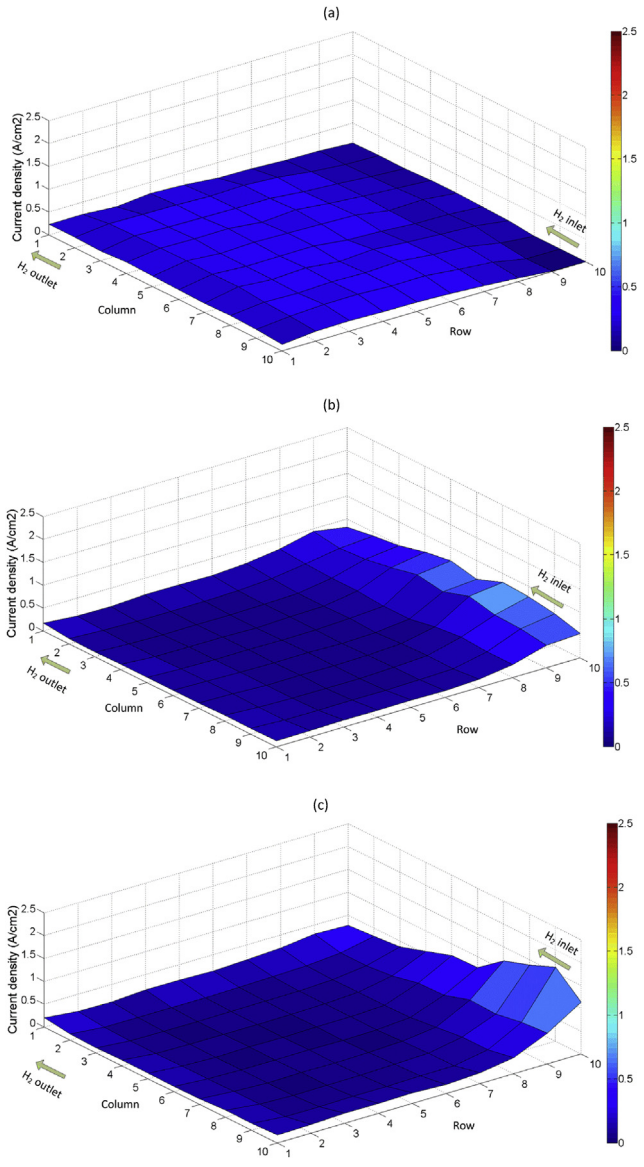

Fig. 5 – Current density distribution profiles of the fuel cell in different time ((a): t = 0 s; (b): t = 16 s when the cell voltage decreases to 0 V; (c): t = 60 s when the cell reversal occurs and the cell voltage reaches the lowest level) during the H_2 starvation process under H_2 stoichiometry of 0.8 and current load of 10 A.

experiment is shown in Fig. 5(a), while Fig. 5(b) and (c) shows the distribution when cell voltage decreased to 0 V and when cell voltage decreased to the lowest level, respectively. It can be seen that at the beginning of the experiment when the fuel cell is operated at normal H_2 stoichiometry condition, the current density is evenly distributed, only with marginal difference in current densities in different regions. In this condition the difference in current density is mainly caused by the inhomogeneous catalyst distribution on the electrode surface during manufacturing process. When the cell voltage decreases to 0 V, obvious heterogeneity in current density distribution is visible, as seen in Fig. 5(b). The current density is highest in the upstream regions. And it decreases along the anode flow channel and becomes the lowest in the downstream regions because of the high mass transfer resistance in the downstream regions caused by H_2 depletion in these regions. The difference between the highest current density and the lowest current density is 0.76 A/cm^2 at this moment. As cell voltage decreases further to the lowest level, the heterogeneity in the current density becomes much more severe. The current density in the upstream regions becomes even higher while in the downstream regions remains in the low level, which increases the difference between the highest value and the lowest current density values to 1.59 A/cm^2. This more severe heterogenous distribution in current density can be attributed to larger area of H_2 depletion when cell voltage decreases, thus current density in more regions becomes extremely low, resulting in most current flowing through the small region near the H_2 inlet. The local high current density could result in local high temperatures, which is another cause for degradation in H_2 starvation conditions besides the carbon corrosion.

The effect of H_2 stoichiometry

The change in cell voltage and local current density when H_2 stoichiometry decreases from 3.0 to 0.4 with the current load of 10 A is measured and illustrated in Fig. 6, to investigate the effect of H_2 stoichiometry to the behaviors of a fuel cell under H_2 starvation conditions. The change in cell voltage in this condition is similar to that in the experiment in which H_2 stoichiometry decreases from 3.0 to 0.8. The difference lies in that the cell voltage decreases earlier and more promptly in this condition. The time needed for the cell reversal and the lowest cell voltage under different operating conditions is listed in Table 2. It takes 19 s for the cell voltage to be reversed in H_2 stoichiometry of 0.8, whereas in H_2 stoichiometry of 0.4 a short time (15 s) is needed. As the H_2 stoichiometry becomes lower, the H_2 depletion rate is faster which causes the faster decay rate in cell voltage. Another difference lies in that the cell reversal is more severe at H_2 stoichiometry of 0.4 than at H_2 stoichiometry of 0.8, as indicated by lower reversed cell voltage shown in Table 2. With lower H_2 stoichiometry, lower

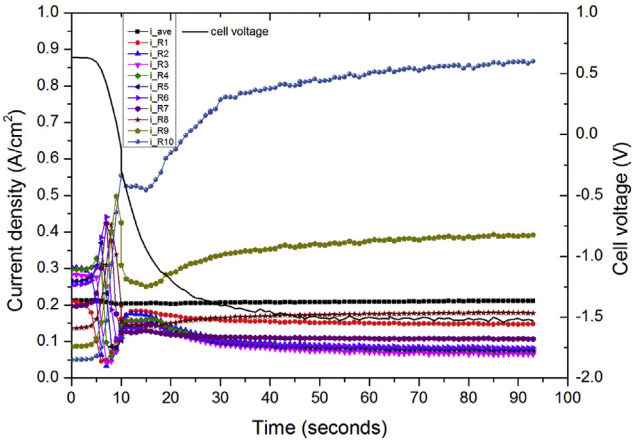

Fig. 6 – Dynamic response of cell voltage and local current density when H_2 stoichiometry decreases from 3.0 to 0.4 with the current load of 10 A.

Table 2 – Values for cell voltage and local current density under different operating conditions.

Operating conditions	Time needed for cell reversal (s)	Reversed cell voltage (V)	Difference between highest and lowest local current density (A/cm^2)[b]
10 A, $\lambda_{H2} = 0.8$	19	−0.75	1.59
10 A, $\lambda_{H2} = 0.4$	15	−1.50	2.45
20 A, $\lambda_{H2} = 0.8$	17	−1.20[a]	2.00
20 A, $\lambda_{H2} = 0.4$	12	−2.30	2.52

[a] This value is the average cell voltage between 40 s and 115 s.
[b] These values are measured when the cell voltage decreased to the lowest value in each experiment.

current is provided by the H_2 oxidation reaction, thus more current should be provided by other reactions such as carbon corrosion and water electrolysis reactions to maintain the constant current in the experimental circuit. Therefore higher anode potential is presented to increase the reaction rates of carbon corrosion and water electrolysis, resulting in lower reversed cell voltage. Given the higher carbon corrosion rate in this experiment, it can be concluded that lower H_2 stoichiometry can bring about more severe degradation in the fuel cell under H_2 starvation condition.

In this experiment the anode exhaust consists of N_2, CO_2 and O_2 as shown in Fig. 4. The existence of O_2 in the anode exhaust indicates the occurrence of water electrolysis. The anode potential at the H_2 stoichiometry of 0.4 is higher than that at the H_2 stoichiometry of 0.8 because of more severe cell reversal, which is high enough to trigger the electrolysis reaction. Moreover, the CO_2 concentration in anode exhaust in the H_2 stoichiometry of 0.4 is higher than that in the H_2 stoichiometry of 0.8, which means the carbon corrosion rate becomes higher with lower H_2 stoichiometry. This can be attributed to higher anode potential. On the other hand, with less H_2 supplied to the anode in this experiment, more current have to be provided by the carbon corrosion and water electrolysis reactions, thus the carbon corrosion rate is higher.

The change in local current density distribution at H_2 stoichiometry of 0.4 shown in Fig. 6 is similar to that at H_2 stoichiometry of 0.8 as well. In the upstream regions the current densities increase while they decline in the downstream regions when the cell voltage drops. However there are obvious overshoots in current densities in the downstream regions and undershoots in current densities in the upstream regions between 10 and 20 s. The reason for this dynamic phenomenon needs further investigation to fully understand the mechanisms involved.

The current density distribution when the H_2 stoichiometry decreases to 0.4 and the cell voltage decreases to the lowest level is illustrated in Fig. 7. As can be seen the local current density values decreases along the flow channel direction. Compared with the current density distribution in H_2 stoichiometry of 0.8, the area with high current density values is much less in H_2 stoichiometry of 0.4. More regions show extremely low current density, indicating the H_2 depletion occurs in more regions. Lower H_2 stoichiometry suggests less H_2 supplied to the anode of the fuel cell, which is the reason

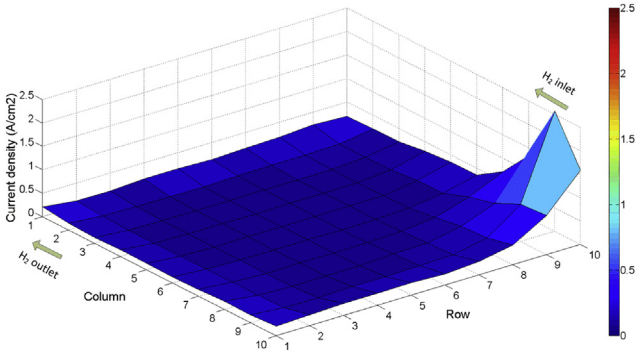

Fig. 7 – Current density distribution profile of the fuel cell when the cell reversal occurs and the cell voltage reaches the lowest level during the H_2 starvation process under H_2 stoichiometry of 0.4 and current load of 10 A.

for larger area with H_2 depletion. Given the fact that the total current flowing through the cell is constant, most current have to flow through a small region near the fuel inlet since in most regions the current is quite low, causing extremely high current density in this region. The difference between the highest and lowest current density is 2.52 A/cm^2 in this case, higher than that in H_2 stoichiometry of 0.8. This indicates that low H_2 stoichiometry could result in higher local current density and consequently higher local temperature, which could further accelerate the degradation.

The effect of current load

To investigate the effect of current load to the cell behaviors under H_2 starvation conditions, the change in cell voltage and local current densities are measured with current load of 20 A and illustrated in Fig. 8. By comparing with Fig. 3, it can be seen that the variation trend in cell voltage is similar with that in current load of 10 A. However the current load can affect the cell voltage drop rate and the reversed cell voltage. As can be seen from Table 2, the cell voltage drops faster with current load of 20 A than with current load of 10 A, which can be attributed to the higher H_2 consumption rate with higher current load. Moreover, the cell reversal is more severe with higher current load. Under sufficient H_2 stoichiometry conditions the ohmic loss as well as polarization losses including activation loss and mass transfer loss are higher with higher current load, resulting in lower cell voltage. Likewise, polarization losses and ohmic loss are higher with higher current under H_2 starvation conditions, resulting in more severe reversed cell voltage. This phenomenon suggests that the degradation caused by H_2 starvation could be more severe with higher current load. It can be noticed from Fig. 8(a) that the cell voltage starts to oscillate when it decreases below 0.5 V. The oscillation in cell voltage can be attributed to the small oscillation in anode flow rate and current load controlled by the test bench.

The change in local current densities is not significantly affected by the current load, except the diverging rate between the current density in different regions becomes higher with higher current load due to higher cell voltage decline rate.

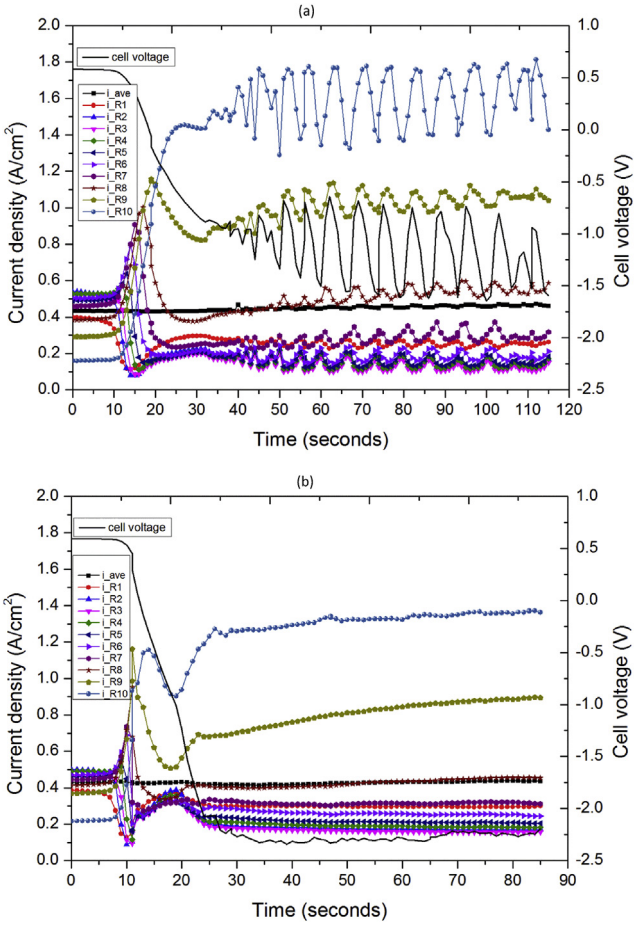

Fig. 8 – Dynamic response of cell voltage and local current density when H_2 stoichiometry decreased to 0.8 (a) and 0.4 (b) with current load of 20 A.

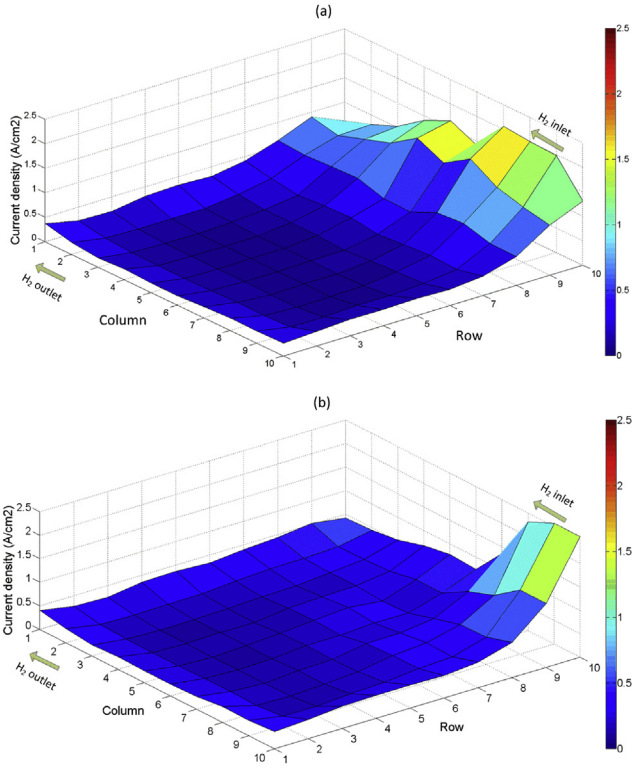

Fig. 9 – Current density distribution profiles of the fuel cell when the cell reversal occurred and the cell voltage reached the lowest level during the H_2 starvation process under H_2 stoichiometry of 0.8 (a) and 0.4 (b) with current load of 20 A.

The anode exhaust compositions under H_2 starvation conditions with current load of 20 A are also shown in Fig. 4. It can be seen that the anode exhaust compositions at the same H_2 stoichiometry are similar for both current loads. At lower current load the CO_2 concentration is lower. The cell reversal is less severe with lower current load, which indicates lower anode potential. Therefore the carbon corrosion reaction rate is lower with lower current load, resulting in the lower CO_2 concentration.

The current density distribution with current load of 20 A is similar to that with current load of 10 A as can be seen from Fig. 9. Most part of current flow through the upstream regions, which makes the current density in these regions higher than that in other regions. In lower H_2 stoichiometry the area with extremely low current density is even larger than that at higher H_2 stoichiometry. However the local current density in the upstream regions is higher with higher current load. The current densities in the downstream regions are quite low with both current loads, thus the current flowing through the upstream regions is higher with higher current load. Therefore, the difference between the highest and lowest current density is higher with higher current load, as shown in Table 2. It can be inferred that the temperature in the upstream regions are higher with higher current load, which could result in more severe degradation.

Conclusion

The cell voltage and local current densities of an HT-PEM fuel cell were measured under H_2 starvation conditions with different H_2 stoichiometries and different current loads in this work. The experimental results show that the cell reversal can be observed under H_2 starvation conditions. With higher current load and lower H_2 stoichiometry, the cell reversal is more severe. Additionally, the current density distribution becomes significantly uneven under H_2 starvation conditions. Current densities in the H_2 upstream regions are higher than those in the H_2 downstream regions. The difference between highest current density and lowest current density increases with higher current load and lower H_2 stoichiometry. During all the experiments, certain amount of CO_2 and O_2 in anode exhaust is detected under H_2 starvation conditions, indicating that the carbon corrosion reaction and water electrolysis reaction occur. With lower H_2 stoichiometry, more O_2 and CO_2 were generated, implying the increased reaction rates of carbon corrosion and water electrolysis. It can be concluded from the results in this work that the H_2 starvation should be

avoided during the operation of the fuel cell to prevent its irreversible damages to the fuel cell.

Acknowledgments

This work was supported by the Danish Energy Technology and Research and Demonstration program under the COBRA-II grant (grant number 64012-0257) and the Danish Strategic Research Council under the 4M grant (Energy and Environment grant 12-132710). Fan Zhou appreciates the financial support from China Scholarship Council (CSC).

REFERENCES

[1] Li Q, Jensen JO, Savinell RF, Bjerrum NJ. High temperature proton exchange membranes based on polybenzimidazoles for fuel cells. Prog Polym Sci 2009;34:449–77.
[2] Chandan A, Hattenberger M, El-kharouf A, Du S, Dhir A, Self V, et al. High temperature (HT) polymer electrolyte membrane fuel cells (PEMFC) – a review. J Power Sources 2013;231:264–78.
[3] Su H, Pasupathi S, Bladergroen B, Linkov V, Pollet BG. Optimization of gas diffusion electrode for polybenzimidazole-based high temperature proton exchange membrane fuel cell: evaluation of polymer binders in catalyst layer. Int J Hydrog Energy 2013;38:11370–8.
[4] Su H, Jao T-C, Pasupathi S, Bladergroen BJ, Linkov V, Pollet BG. A novel dual catalyst layer structured gas diffusion electrode for enhanced performance of high temperature proton exchange membrane fuel cell. J Power Sources 2014;246:63–7.
[5] Ong A-L, Jung G-B, Wu C-C, Yan W-M. Single-step fabrication of ABPBI-based GDE and study of its MEA characteristics for high-temperature PEM fuel cells. Int J Hydrog Energy 2010;35:7866–73.
[6] Andreasen SJ, Kær SK. Modelling and evaluation of heating strategies for high temperature polymer electrolyte membrane fuel cell stacks. Int J Hydrog Energy 2008;33:4655–64.
[7] Mamlouk M, Scott K. The effect of electrode parameters on performance of a phosphoric acid-doped PBI membrane fuel cell. Int J Hydrog Energy 2010;35:784–93.
[8] Kang J, Jung DW, Park S, Lee J-H, Ko J, Kim J. Accelerated test analysis of reversal potential caused by fuel starvation during PEMFCs operation. Int J Hydrog Energy 2010;35:3727–35.
[9] Taniguchi A, Akita T, Yasuda K, Miyazaki Y. Analysis of electrocatalyst degradation in PEMFC caused by cell reversal during fuel starvation. J Power Sources 2004;130:42–9.
[10] Liang D, Dou M, Hou M, Shen Q, Shao Z, Yi B. Behavior of a unit proton exchange membrane fuel cell in a stack under fuel starvation. J Power Sources 2011;196:5595–8.
[11] Liang D, Shen Q, Hou M, Shao Z, Yi B. Study of the cell reversal process of large area proton exchange membrane fuel cells under fuel starvation. J Power Sources 2009;194:847–53.
[12] Yousfi-Steiner N, Moçotéguy P, Candusso D, Hissel D. A review on polymer electrolyte membrane fuel cell catalyst degradation and starvation issues: causes, consequences and diagnostic for mitigation. J Power Sources 2009;194:130–45.
[13] Orfanidi A, Daletou M, Sygellou L, Neophytides S. The role of phosphoric acid in the anodic electrocatalytic layer in high temperature PEM fuel cells. J Appl Electrochem 2013;43:1101–16.
[14] Baumgartner W, Parz P, Fraser S, Wallnöfer E, Hacker V. Polarization study of a PEMFC with four reference electrodes at hydrogen starvation conditions. J Power Sources 2008;182:413–21.
[15] Pérez LC, Brandão L, Sousa JM, Mendes A. Segmented polymer electrolyte membrane fuel cells—a review. Renew Sustain Energy Rev 2011;15:169–85.
[16] Zhang G, Shen S, Guo L, Liu H. Dynamic characteristics of local current densities and temperatures in proton exchange membrane fuel cells during reactant starvations. Int J Hydrog Energy 2012;37:1884–92.
[17] Yu Y, Yuan X-Z, Li H, Gu E, Wang H, Wang G, et al. Current mapping of a proton exchange membrane fuel cell with a segmented current collector during the gas starvation and shutdown processes. Int J Hydrog Energy 2012;37:15288–300.
[18] Mitsuda K, Murahashi T. Air and fuel starvation of phosphoric acid fuel cells: a study using a single cell with multi-reference electrodes. J Appl Electrochem 1991;21:524–30.
[19] Song R-H, Kim C-S, Shin DR. Effects of flow rate and starvation of reactant gases on the performance of phosphoric acid fuel cells. J Power Sources 2000;86:289–93.
[20] Zhou F, Andreasen SJ, Kær SK, Yu D. Analysis of accelerated degradation of a HT-PEM fuel cell caused by cell reversal in fuel starvation condition. Int J Hydrog Energy 2015;40:2833–9.
[21] Larminie J, Dicks A, McDonald MS. Fuel cell systems explained. New York: Wiley; 2003.